Simultaneous selection by object-based attention in visual and frontal cortex

Arezoo Pooresmaeili[a,1], Jasper Poort[a,2], and Pieter R. Roelfsema[a,b,c,3]

[a]The Netherlands Institute for Neuroscience, Royal Netherlands Academy of Arts and Sciences, 1105 BA, Amsterdam, The Netherlands; [b]Department of Integrative Neurophysiology, Centre for Neurogenomics and Cognitive Research, VU University Amsterdam, 1081 HV, Amsterdam, The Netherlands; and [c]Psychiatry Department, Academic Medical Centre, University of Amsterdam, 1105 AZ, Amsterdam, The Netherlands

Edited by Michael E. Goldberg, Columbia University College of Physicians and Surgeons, New York, NY, and approved March 12, 2014 (received for review November 15, 2013)

Models of visual attention hold that top-down signals from frontal cortex influence information processing in visual cortex. It is unknown whether situations exist in which visual cortex actively participates in attentional selection. To investigate this question, we simultaneously recorded neuronal activity in the frontal eye fields (FEF) and primary visual cortex (V1) during a curve-tracing task in which attention shifts are object-based. We found that accurate performance was associated with similar latencies of attentional selection in both areas and that the latency in both areas increased if the task was made more difficult. The amplitude of the attentional signals in V1 saturated early during a trial, whereas these selection signals kept increasing for a longer time in FEF, until the moment of an eye movement, as if FEF integrated attentional signals present in early visual cortex. In erroneous trials, we observed an interareal latency difference because FEF selected the wrong curve before V1 and imposed its erroneous decision onto visual cortex. The neuronal activity in visual and frontal cortices was correlated across trials, and this trial-to-trial coupling was strongest for the attended curve. These results imply that selective attention relies on reciprocal interactions within a large network of areas that includes V1 and FEF.

contour grouping | noise correlation | error trials

Visual scenes are usually too complex for all information to be analyzed at once. Selective attention selects a subset of the objects in the visual scene for detailed analysis at the expense of other items. Visual objects compete for selection, and the outcome of this competition depends on bottom-up cues such as saliency and perceptual organization and top-down cues that signal the objects' behavioral relevance (1). It is not well understood how these different cues interact and which brain areas take the lead in visual selection.

The top-down mechanisms for attentional selection are tightly linked to those for the selection of actions (2), and accordingly, cortical areas related to action planning influence the deployment of visual attention. The frontal eye fields (FEF) is one such area that is involved in visual processing, shifts of visual attention (2, 3), and also in the control of eye movements (4, 5). Area FEF contains different types of cells. Visual processing relies on visual and visuomovement cells, whereas the programming of eye movements relies on the activity of visuomovement and movement cells (6, 7). There are several lines of evidence that also implicate FEF in attentional control. First, FEF inactivation impairs attention shifts toward the contralateral visual field (8, 9). Second, subthreshold FEF microstimulation enhances neuronal activity in visual cortex in a manner that is reminiscent of selective attention (10, 11). Third, a role of FEF in the top-down guidance of attention is supported by studies on visual search. In search, selection signals in frontal cortex precede those in area V4 by 50 ms, suggesting that the frontal cortex determines selection and then provides feedback to visual cortex (12, 13). A comparable interareal delay in attentional effects was observed between the lateral intraparietal area and the motion sensitive middle temporal area (14). Thus, the parietal and frontal cortices appear to take the lead in attentional selection and to provide top-down signals to visual cortex. Within the visual cortex, such a reverse hierarchy (15) of attentional effects was observed in a task that required shifts of spatial attention (16) and also in a task demanding shifts between visual and auditory attention (17). Attentional signals in area V4 preceded signals in V2 by 50–250 ms, which in turn preceded attentional effects in the primary visual cortex (V1) by 50–400 ms.

However, top-down factors are not the only ones that guide attention. Attention can be object-based, implying that the visual stimulus itself influences the distribution of attention too. If attention is directed to a feature, attention tends to coselect visually related features on the basis of perceptual grouping cues (18) so that entire objects rather than isolated features are attended (19, 20). The influence of perceptual grouping on attentional selection can be investigated with a curve-tracing task that requires grouping of the contour elements of a single curve (21, 22). Attention in this task is directed to the entire curve, implying that the curve's shape itself influences the distribution of attention (22). Indeed, a traced curve evokes stronger activity in primary visual cortex than an irrelevant curve, revealing a neuronal correlate of object-based attention (23). However, it is not known if the coselection of all image elements of a single object is determined within early visual cortex or is guided by the frontal cortex, just as was shown for other tasks.

Here we compare selection signals in areas FEF and V1 in the curve-tracing task with simultaneous recordings in the two areas. A priori, several possibilities exist for the interaction between V1

Significance

Visual attention allows us to focus on information that is relevant to our goals and to discard irrelevant information. The brain mechanisms that steer attention are only partially understood, but previous research suggested that the frontal cortex controls activity in the visual cortex. We here demonstrate that attentional signals in visual and frontal cortex of the macaque monkey emerge at the same time in a curve-tracing task, suggesting a more active participation of visual cortex. If attentional signals in visual cortex were weak, frontal cortex took the lead, but errors were likely. In these error trials, frontal cortex imposed its decision on visual cortex. Our results reveal how visual and frontal cortex interact to control attention.

Author contributions: A.P., J.P., and P.R.R. designed research; A.P. and J.P. performed research; A.P. and J.P. analyzed data; and A.P. and P.R.R. wrote the paper.

The authors declare no conflict of interest.

This article is a PNAS Direct Submission.

Freely available online through the PNAS open access option.

[1]Present address: Berlin School of Mind and Brain, Humboldt University, 10117 Berlin, Germany.

[2]Present address: Department of Neuroscience, Physiology and Pharmacology, University College London, London WC1E 6DE, United Kingdom.

[3]To whom correspondence should be addressed. E-mail: p.roelfsema@nin.knaw.nl.

This article contains supporting information online at www.pnas.org/lookup/suppl/doi:10.1073/pnas.1316181111/-/DCSupplemental.

and FEF. First, the frontal cortex might select the relevant curve and then feed a guiding signal back to visual cortex (24, 25) as in the other tasks described above. If so, attentional selection signals in V1 might arise tens to hundreds of milliseconds later than in FEF. However, the chain of events in the curve-tracing task might differ because visual shape has a profound influence on the distribution of attention (26). Thus, a second possibility is that the visual cortex determines selection so that the attentional modulation in visual cortex precedes that in frontal cortex. A third possibility is that visual and frontal areas jointly determine what is relevant and what is not. In this situation, the selection signals are expected to occur in both areas at approximately the same time. It is also possible that the order of selection in different areas depends on the difficulty of the task. For example, the reverse hierarchy theory of visual perception (15) proposed that easy tasks are usually solved by higher visual areas, whereas lower visual areas are recruited when the picture has to be scrutinized. We therefore varied the difficulty of the curve-tracing task.

Results

Two monkeys carried out the curve tracing task illustrated in Fig. 1*A*. A trial started when the monkey directed his gaze to a fixation point. After 300 ms, two curves with two circles at their ends appeared on the screen. One of the curves was connected to the fixation point (target curve, T), whereas the other curve was not (distractor, D). The monkeys maintained fixation while mentally tracing the target curve to locate the circle at the end of this curve. After 500 ms the fixation point disappeared, cuing the monkey to make an eye movement. We rewarded eye movements toward the circle at the end of the target curve and counted saccades to the other circle as errors. We manipulated the task difficulty by varying the luminance of the short initial segment of the target curve (Fig. 1*B*). This segment could have

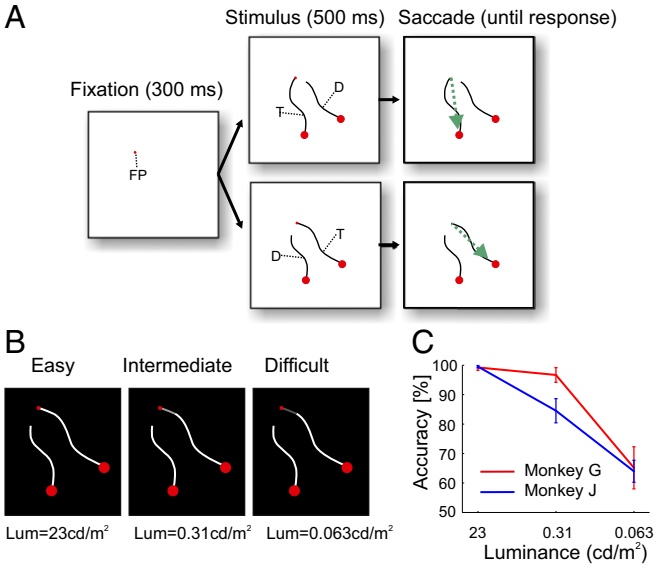

Fig. 1. Curve tracing task and behavioral performance. (*A*) The monkey first directed gaze to a small fixation point (FP). After 300 ms, two curves appeared on the screen. The curve that is connected to the fixation point is the target curve (T), and the other curve is a distractor (D). After 500 ms the fixation point disappeared, and the monkey made an eye movement to the circle that had been connected to the fixation point. (*B*) The difficulty of the task was varied by changing the luminance of the short contour element that connected the target curve to the fixation point (the luminance in the difficult condition was even lower than shown here). (*C*) Accuracy of the two monkeys as a function of the luminance of the connecting segment. The accuracy decreased if the connecting segment had a lower luminance.

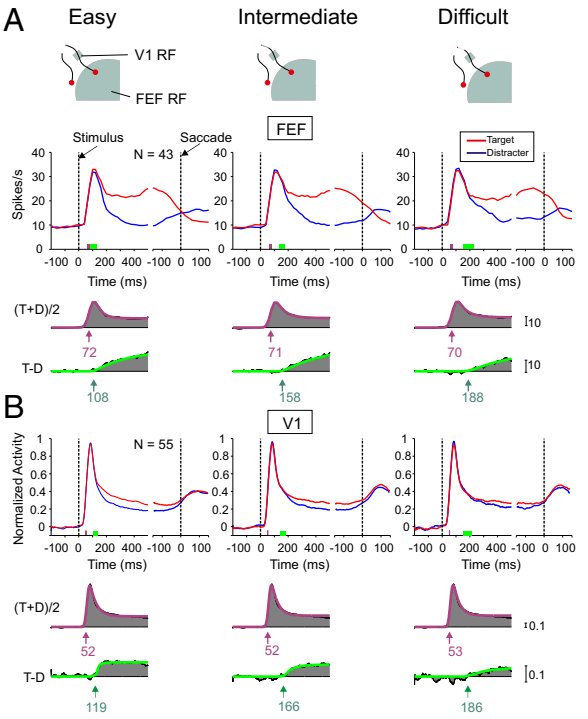

Fig. 2. Population responses in FEF and area V1. (*A* and *B*) The average responses of all neurons in FEF (*A*) and area V1 (*B*). The red and blue traces show the responses evoked by the target and distractor curve, respectively. In both *A* and *B*, *Lower* panels show the average visual response and the attentional response modulation. Curves were fitted to estimate the latency of the visual response (purple) and response modulation (green). Rectangles on the *x* axis show the estimated latency ±1 sd (determined with bootstrapping). On the right side of the graphs, the PSTHs were aligned on the saccade onset.

one of three luminances. In the easy condition it was 23 cd/m^2, equal to the rest of the curve. It was 0.31 cd/m^2 in the intermediate condition and 0.063 cd/m^2 in the most difficult condition (background luminance was 0.026 cd/m^2). As expected, the performance of both monkeys decreased for lower luminances because it became more difficult to distinguish the target curve from the distractor (Fig. 1*C*). In the easy condition the average accuracy of the two monkeys was 99%; it decreased to an average of 90% in the intermediate condition and to 64% in the difficult condition (repeated-measures ANOVA; monkey G: $F_{2,24} = 71.2$; monkey J: $F_{2,64} = 162$; both $Ps < 10^{-6}$).

Strength of Attentional Modulation in FEF and V1. In every recording session, we isolated a single unit in area FEF and monitored multiunit activity in area V1 at the same time with chronically implanted electrode arrays. We obtained simultaneous recordings from a total of 56 single units (SUA) in FEF (23 in monkey G and 33 in monkey J) and 55 multiunit (MUA) recording sites in V1 (21 in monkey G and 34 in monkey J). In our population analysis of FEF we only included visual and visuomovement cells while excluding movement cells (43 FEF neurons remained: 13 in monkey G and 30 in monkey J). Fig. 2 shows the population responses in FEF and V1, obtained by averaging activity across neurons in the two areas (for an example session, see *Supporting Information*). Attentional response modulation was significant in both areas and at every level of task difficulty (Wilcoxon signed-rank test in a window from 200 to 500 ms, all $Ps < 0.01$). We quantified the response modulation with a modulation index (MI; [target − distractor]/average, 200–500 ms after stimulus onset). The MI decreased as the task became more difficult. In FEF, the average MI was 0.62 in the easy condition, 0.47 in the intermediate condition, and 0.31 in

the difficult condition (Fig. 3*A*). The MI in the difficult condition was significantly lower than in the easy and intermediate conditions ($Ps < 0.01$, Wilcoxon signed-rank test), but the difference between the easy and intermediate conditions was not significant ($P > 0.05$). In area V1, the average MI was 0.25 in the easy condition; it decreased to 0.22 in the intermediate condition and to 0.12 in the difficult condition (Fig. 3*B*) (all $Ps < 10^{-5}$, Wilcoxon signed-rank test).

We also compared the strength of the attentional modulation between the two areas (Fig. 3) and found that the MI in V1 was significantly smaller than that in FEF (Mann–Whitney u test, $P < 10^{-2}$ at all difficulty levels). It seems unlikely that this difference is due to the distinct recording methods (MUA in V1 vs. single units in FEF), for a number of reasons. First, the MI of MUA equals a weighted average of the MIs of the contributing neurons, and it is therefore valid to compare the MI of single units to that of MUA. Second, the signal-to-noise ratio of the visual response in V1 (median d-prime = 2.9) was significantly larger than that of single units and MUA in FEF (SUA median d-prime = 0.93; MUA, 1.8; both $Ps < 10^{-3}$, Mann–Whitney u test). In contrast, the signal-to-noise ratio of the attentional modulation was higher in FEF. In FEF the d-prime of attentional modulation in the easy condition had a median of 0.72 for SUA and 1.18 for MUA, significantly larger than the attention d-prime in V1 with a median of 0.5 (both $Ps < 10^{-2}$, Mann–Whitney u test). These findings confirm our MI analysis; visual responses are more reliable in V1, whereas attentional modulation is stronger in FEF. Indeed, it can be seen in Fig. 2 that the representation of the distractor curve is strongly suppressed in FEF, whereas V1 continues to represent both curves and therefore has weaker attentional modulation.

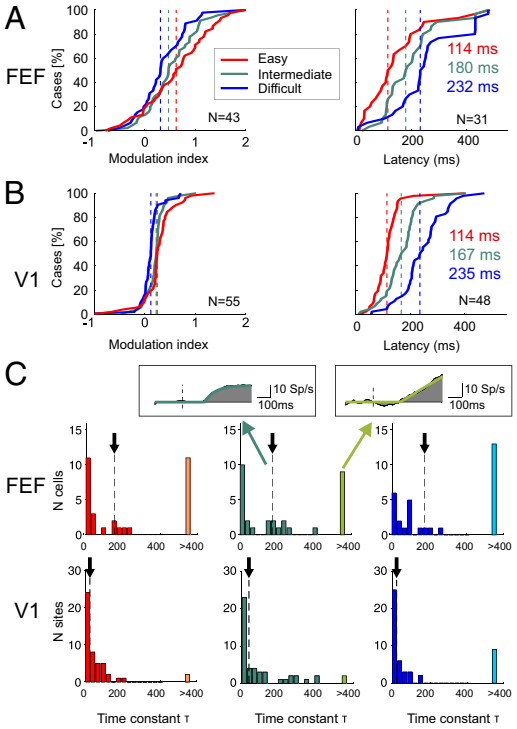

Fig. 3. Magnitude and latency of response modulation of individual FEF cells and V1 recording sites. (*A*) The distribution of the modulation index (*Left*; $n = 43$) and latency of attentional modulation (*Right*) across the population of FEF cells ($n = 31$ cells with a reliable latency measurement). The blue, green, and red traces correspond to the difficult, intermediate, and easy conditions, respectively. The vertical dashed lines are the medians of the distributions. (*B*) The cumulative distribution of MI (*Left*; $n = 55$) and attentional modulation latency (*Right*) across the V1 recording sites ($n = 48$ sites with reliable latency measurements). (*C*) Distribution of the time constant of the modulation τ, at the easy (*Left*), intermediate (*Center*), and difficult (*Right*) levels in FEF and V1. The insets show the temporal profiles of the modulation of 18 cells with $\tau < 400$ ms (*Left*) and 13 cells with $\tau > 400$ ms (*Right*).

Latency of the Visual Response and Attentional Modulation in V1 and FEF. The latency of the average visual response in V1 was 52 ± 2 ms (s.d. determined with bootstrap analysis), significantly earlier than the visual response of visual and visuomovement cells in FEF at a latency of 71 ± 10 ms (bootstrap test, $P < 0.05$), in accordance with a previous study (27) (purple fits in Fig. 2; *Supporting Information*). Thus, the visual response is earlier in V1 than in FEF.

The initial neuronal responses in either area did not discriminate between the target and the distractor curve, but after a delay the responses evoked by the target curve became stronger than those evoked by the distractor (23, 27). To estimate the attentional latency, we used a curve-fitting method (green fits in Fig. 2), which does not depend on modulation strength (unlike methods based on significance). We estimated the temporal profile of attentional modulation with an exponential function $f(t)$, which gave good fits:

$$\begin{cases} f(t) = 0, & ; \quad t < t_0 \\ f(t) = a(1 - \exp(-(t - t_0)/\tau)); & t \geq t_0. \end{cases} \quad [1]$$

Here a is the maximal modulation amplitude, τ is a time constant that determines the rate of increase, and t_0 is the latency.

The attentional latency in FEF was 108 ms in the easy condition, and it increased to 158 ms and 188 ms in the intermediate and difficult conditions, respectively (bootstrap test, all $Ps < 0.05$) (Fig. 2*A*). In area V1, the latency of the attentional modulation in the easy condition was 119 ms; it increased to 166 ms in the intermediate condition and to 186 ms in the difficult condition (bootstrap tests, $Ps < 0.05$, except the intermediate vs. difficult condition with $P > 0.2$). The attentional latency did not differ between areas at any difficulty level (bootstrap test, $Ps > 0.05$ in all conditions). This finding held for both visual and visuomovement neurons in FEF and was also true when we compared MUA in both areas (*Supporting Information*). Thus, the similar attentional latency in V1 and FEF is not caused by the heterogeneity of FEF cell types or the comparison of single units to MUA.

Latency Distributions in V1 and FEF. We next investigated the latency distribution across recordings (Fig. 3 *A* and *B*). The median latency of the attentional modulation in FEF was 114 ms (mean ± SD: 144 ± 21 ms) in the easy condition; it increased to 180 ms (mean 194 ± 19 ms) in the intermediate condition and to 232 ms (249 ± 23 ms) in the difficult condition (all $Ps < 10^{-4}$, Wilcoxon signed-rank test). In area V1, the median latency of the attentional modulation was 114 ms (mean 115 ± 8 ms) in the easy condition; it increased to 167 ms (164 ± 10 ms) in the intermediate condition and to 235 ms (241 ± 11 ms) in the difficult condition (all $Ps < 10^{-5}$). Again, there were no significant differences between areas at any difficulty level (Mann–Whitney u test, all $Ps > 0.05$).

We replicated these results when we analyzed the data of the two monkeys separately. In monkey G, the attentional latencies in FEF were 119 ± 17 ms, 157 ± 16 ms, and 192 ± 39 ms, and in V1 they were 116 ± 18 ms, 156 ± 25 ms, and 188 ± 28 ms in the easy, intermediate, and difficult conditions, respectively (comparison of V1 and FEF: at all difficulty levels, $P > 0.05$, Mann–Whitney u test). In monkey J, the latencies in FEF were 111 ± 44 ms, 166 ± 54 ms, and 221 ± 81 ms, and in V1 they were 118 ± 17 ms, 171 ± 18 ms, and 222 ± 35 ms (all $Ps > 0.05$). Thus, we observed small and nonsignificant differences in the attentional latency between V1 and FEF, although latency increased with task difficulty in both areas.

In our sample, the average eccentricity of the FEF receptive fields (RFs) was 12.3°, which was larger than the average eccentricity of the V1 RFs of 2.5°. We considered the possibility

that the latency of the attentional response modulation increases with eccentricity because it might take time for attention to spread along the curve to the more eccentric RFs. We therefore computed the correlation between attentional latency and RF eccentricity, but it was not significant in V1 ($\rho = 0.001$, $P > 0.2$) or FEF ($\rho = 0.18$, $P > 0.2$). Thus, the similar attentional latency was not caused by a difference in RF eccentricity.

Temporal Profile of Attentional Modulation in V1 and FEF. Although the attentional latency is similar in the two areas, we noticed that the V1 modulation saturates during a phase where FEF modulation is still increasing (compare green curves in Fig. 2). To further explore this difference between areas, we computed the MI in a late time window (400–500 ms) and compared it to that in an earlier window (200–300 ms). In FEF, but not in V1, the MIs in the late window were significantly larger than those in the earlier window (FEF: all *Ps* < 0.05; V1: all *Ps* > 0.3, Wilcoxon signed-rank test at each level of difficulty). Thus, the attentional modulation reaches a plateau in V1 but keeps increasing in FEF. This effect is also reflected in the time constant τ in Eq. **1**, which estimates the rate of increase in modulation (Fig. 3*C*). The median τ across FEF neurons was 144 ms in the easy condition, 165 ms in the intermediate condition, and 167 ms in the difficult condition. The corresponding values in V1 were 12 ms, 25 ms, and 12 ms. The time constant τ was significantly larger in FEF than in V1 at every difficulty level ($P < 0.05$, Mann–Whitney *u* test). A large fraction of FEF neurons had τ values larger than 400 ms, and their activity increased until the saccade.

Representation of Erroneous Choices in Areas FEF and V1. We next investigated neuronal activity in trials where the monkey selected the wrong curve. We restricted this analysis to the difficult configuration, where both animals made a substantial number of errors (more than five per session). Fig. 4 compares the average activity of FEF and V1 neurons in error trials to that in correct trials. In error trials, the attentional response modulation in area FEF was reversed. Now the responses evoked by the distractor curve were significantly stronger than responses evoked by the target (Wilcoxon signed-rank test, $P < 0.005$). The strength of this reversed modulation in FEF was similar to the response modulation on correct trials ($P > 0.7$, Wilcoxon signed-rank test). Moreover, the latency of response modulation on error trials (mean 192 ms) was similar to the latency on correct trials (bootstrap test, $P > 0.8$). Thus, FEF cells faithfully reflected the monkey's behavioral choice, irrespective of whether it was correct or erroneous.

In area V1, neuronal activity evoked by the distractor curve was also stronger than that evoked by the target on error trials ($P < 0.01$, Wilcoxon signed-rank test). In V1 the reversed modulation occurred at 297 ± 62 ms, which was significantly later than the latency of 186 ms in correct trials (bootstrap test, $P < 10^{-3}$). A comparison of latencies in error trials revealed a further difference between the two areas. Erroneous choices were represented at a shorter latency in FEF than in V1 (bootstrap test, $P < 10^{-3}$), at the population level and for each monkey separately (monkey G, $P < 10^{-5}$; monkey J, $P < 0.05$). Apparently, FEF took the lead in the error trials. This erroneous selection was imposed on V1 but after a substantial delay.

Coupling of Neuronal Activity in FEF and V1. The finding that FEF and V1 both select the wrong curve in those trials where the monkey made a mistake implies a coupling of neuronal activity between areas. As a further measure for coupling we computed the correlation between the trial-to-trial fluctuations in activity (noise correlation) (Fig. 5*A*). If the V1 RF and the FEF RF both fell on the target curve ($n = 129$ paired recordings), the average correlation was 0.05, which was significantly larger than zero ($P < 0.0001$, Wilcoxon signed-rank test). However, if both RFs fell on the distractor curve, the average correlation coefficient was only 0.008,

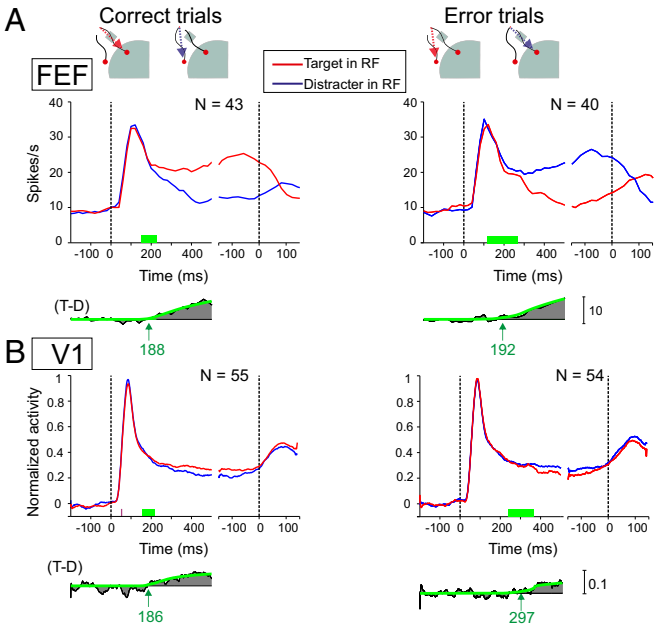

Fig. 4. Neuronal activity in FEF and V1 on error trials. (*A* and *B*) Population response of FEF cells (*A*) and V1 sites (*B*) during correct (*Left*) and erroneous (*Right*) trials in the difficult condition (the visibility of the connecting segment in the inset has been enhanced for clarity). The red and blue traces correspond to the responses evoked by the target and distractor curves, respectively. Note that the attentional modulation is inverted in error trials and delayed in V1.

significantly lower ($P < 10^{-2}$, Wilcoxon signed-rank test). Thus, the interareal coupling is strongest for attended curves.

We also recorded from 258 cases with V1 and FEF RFs on different curves. In this configuration we averaged across the two attention conditions because if one RF fell on the target curve, the other one fell on the distractor. The average noise correlation was 0.023, significantly larger than zero ($P < 0.0005$, sign test) (Fig. 5*A*). The noise correlation was lower when the RFs fell on different curves than if they fell on the target curve ($P < 10^{-2}$, Mann–Whitney *u* test).

We next measured the noise correlation within V1 (666 and 513 pairs with RFs on the same and different curves, respectively; Fig. 5*B*). When the V1 RFs fell on the target curve, the average correlation was 0.118, and it was 0.121 if they fell on the distractor curve, a difference that was not significant ($P > 0.2$, Wilcoxon signed-rank test). When the RFs fell on different curves, the average correlation was 0.07, which was significantly lower ($P < 0.001$, Mann–Whitney *u* test). The correlations within V1 were stronger than between V1 and FEF (Mann–Whitney *u* test, $P < 0.05$), which is expected given the large distance between these areas. Thus, neuronal activity is weakly coupled between V1 and FEF, a coupling that is strongest for the target curve.

We performed two control analyses to verify these results. First, the comparison between same and different curves involved different pairs of recording sites, which may have had different RF distances. However, when RF distances were equalized with a stratification method, noise correlations were still higher if the RFs fell on the same curve both within area V1 and between V1 and FEF (all *Ps* < 0.01, Mann–Whitney *u* test). Second, the stronger V1–FEF noise correlation evoked by the target curve might have been caused by the stronger activity elicited by the target curve. However, when response magnitudes were balanced across attention conditions (*Supporting Information*), noise correlations were still stronger for the target curve.

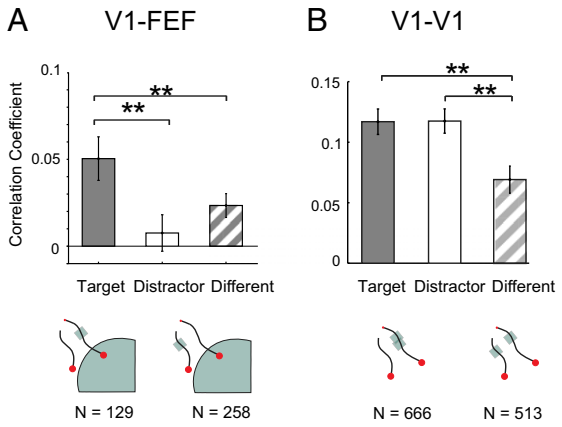

Fig. 5. Noise correlations between FEF and V1 and within V1. (*A*) Noise correlation between FEF and V1 for neurons with RFs on the target curve (gray), distractor curve, or different curves (striped). (*B*) Noise correlations within V1 (**$P < 0.001$).

Eye Position Controls. To investigate whether there were systematic differences in the eye position around the fixation point between conditions with a target or distractor inside RF, we projected single-trial eye positions on an axis that connected the average eye position in the two attention conditions. There were no significant eye position differences in any of the recording sessions (all $Ps > 0.05$, paired t test). Thus, variations in eye position across trials are an unlikely explanation for the results.

Discussion

The present study is the first to our knowledge to simultaneously record the activity of neurons in FEF and V1, at opposite ends of the visual cortical processing hierarchy. We used a curve-tracing task and varied the difficulty of attentional selection. We observed that increases in difficulty reduced the strength of the attentional response modulation and increased the latency of the selection signal, in accordance with previous studies in V1 (28, 29) and FEF (30–32). In correct trials, we did not find consistent differences in the onset of attentional response modulation between visual and frontal cortex, which suggests that these remote brain regions engage in reciprocal interactions during the selection of the target curve. However, in error trials, FEF selected the wrong curve in a phase where attentional modulation in V1 was virtually absent. Apparently, FEF took the lead, and it then imposed the wrong decision on visual cortex. The coselection of the same curve in correct and error trials implies that activity in the two areas is coupled, and this coupling was also observed in the pattern of noise correlations, which were strongest for the attended curve.

Methodological Considerations. In area V1 we recorded multiunit activity, whereas we isolated single units in FEF. It is unlikely that this difference in the recording method is responsible for the pattern of results that we observed. We used the MI to quantify the strength of the modulation, which is the ratio between the difference in activity caused by an attention shift and the average firing rate. This ratio is expected to be the same for single units and MUA. Furthermore, we used a curve-fitting method to determine the latency of the visual response and the attentional response modulation. The advantage of this method (33, 34) is that the latency estimate does not depend on the strength of the modulation, the number of trials, or the number of cells that are measured at a recording site. During FEF single-cell recordings we also recorded FEF-MUA, and we replicated our results with this method (*Supporting Information*).

Flow of Information Between FEF and V1 During Attentional Selection. Previous studies used visual search and spatial cuing tasks to compare the time course of attention shifts between areas. Selection first occurred in frontal and parietal cortex, and the selection signals only arrived in extrastriate visual cortex after a delay of ∼50 ms (12–14, 35). Other studies reported that it also takes time for attentional signals to propagate from V4 to V2 and then back to V1, with delays up to hundreds of milliseconds (16, 17). Combining these results, one would predict that attentional selection in area V1 lags selection in FEF by at least 150 ms. Such a lag would be in support of a reverse hierarchy theory (15) in which frontoparietal areas provide the source of attentional control signals to the visual cortex (25). However, the source of attentional selection signals depends on task demands. A previous study reported that the timing of selection differs between a pop-out visual search task in which attentional selection in parietal cortex preceded selection in frontal cortex (but see 32) and a serial search task in which selection occurred in the opposite order (35).

Human observers that carry out the curve-tracing task start by attending the first segment of the target curve, and they spread attention over the curve until all of its contour elements are attended (21, 22). This process of contour grouping could be implemented in the visual cortex by the spread of enhanced neuronal activity across neurons that code the contour elements of the target curve. The propagation of the enhanced activity could take advantage of the selectivity of corticocortical connections (26) that link neurons coding nearby and collinear contour elements (20, 21, 36). One might therefore also have expected that early visual areas take the lead in selection and that the selection of the relevant eye movement in FEF follows. Instead, we found that selection in both areas was nearly simultaneous.

Although the onset of the selection signals in visual and frontal cortex was similar, the time courses differed. In FEF, the selection signal kept increasing until the time of the saccade, but it saturated earlier in V1. Previous studies suggested that FEF neurons integrate evidence to reach a saccadic decision (2, 37). In the curve-tracing task, the evidence might consist of attentional modulation in visual cortex, which distinguishes the target curve from the distractor. In such a model, FEF would integrate attentional modulation in visual cortex, to select the endpoint of the target curve which is consistent with our finding that the selection signal in FEF keeps increasing when the V1 modulation has saturated.

Another important difference between V1 and FEF occurred in error trials. In both areas the attentional modulation was reversed, but there now was a remarkable delay between frontal and visual cortex as if the frontal cortex took a decision in the absence of attentional modulation in V1. This error was fed back to V1 with a delay of more than 100 ms (Fig. 4), compatible with previously reported delays in visual search and spatial cuing tasks (12–14, 35). Thus, if attentional signals in the visual cortex are weak, frontal cortex appears to enforce a decision and to feed this decision back to the visual cortex.

Coupling Between Neuronal Activity in FEF and V1. The present results show, for the first time to our knowledge, that noise correlations exist between visual and frontal cortex and that they are strongest for the target curve. Thus, object-based attention increases the coupling between remote brain areas, an effect that may be caused by trial-to-trial fluctuations in the process that selects the target curve. Attention did not influence the strength of the noise correlation in V1, in accordance with previous studies with the curve-tracing task (28, 38). This finding contrasts with previous studies reporting that attention reduces noise correlations (39–41), a discrepancy that may reflect a difference between tasks.

The Timing of Attentional Operations in Multistep Tasks. We here showed that attentional selection in the curve tracing task occurs at approximately the same time in visual and frontal cortex, and

previous studies demonstrated that selection in the frontal cortex precedes selection in the visual cortex during visual search (42). What happens if a task requires multiple attentional operations? A recent study required monkeys to first trace a curve, to register the color of a cue at the end of this curve, and to then carry out a visual search for another circle with the same color as the cue. In this task, V1 neurons first selected the relevant curve, but there was a delay that could increase to more than 200 ms before V1 neurons selected the target of search (43). Thus, a single area can contribute to the various processing steps of a complex task at different times. The present results are complimentary, by showing that one such step can be monitored in different areas at approximately the same time. The present and previous results, taken together, therefore provide new insights into the cortical organization of attentional selection, which relies on the coordinated effort of multiple interacting cortical areas, jointly contributing to the successive processing steps of a cognitive task.

Materials and Methods

Two monkeys participated in the experiment. The experiments complied with the National Institutes of Health Guide for Care and Use of Laboratory Animals and were approved by the Institutional Animal Care and Use Committee of the Royal Netherlands Academy of Arts and Sciences.

Behavioral Task. The stimuli consisted of two white curves and two red circles at the end of each curve on a dark gray background (luminance 0.026 cd/m^2). One of the curves was connected to the FP and served as a target curve (T in Fig. 1*A*), whereas the other, unconnected curve was a distractor (D). After a fixation epoch of 500 ms, the FP disappeared, cuing the monkey to make a saccade to the end of the target curve. We manipulated task difficulty by varying the luminance of the contour that connected the target curve to the fixation point (further details are given in *Supporting Information*).

Data Analysis and Statistics. Across sessions, we collected on average 92 correct trials for the easy condition, 83 correct trials for the intermediate condition, and 61 trials for the difficult condition. The strength of attentional effect in V1 sites and FEF single units was quantified with a modulation index defined as $MI = (\mu_T - \mu_D)/((\mu_T + \mu_D)/2)$, where μ_T is the average response to the target curve and μ_D is the average response to the distractor curve from 200 to 500 ms after stimulus onset. We also computed *d*-prime values as $d' = (\mu_1 - \mu_2)/\sigma$. For the *d*-prime of the visual response, μ_1 is activity from 0 to 300 ms (pooled across attention conditions), and μ_2 is spontaneous activity 300 ms before stimulus onset; σ is the pooled SD. For the attentional *d*-prime, μ_2 and μ_1 are activity levels evoked by the target and distractor curves. Significance of attentional modulation was assessed with a Wilcoxon signed-rank test across V1 MUA recording sites and single units in FEF. Comparisons between areas were carried out with the Mann–Whitney *u* test. The methods used to measure the latency of the visual response and the attentional modulation and the noise correlation have been described in *Supporting Information*.

ACKNOWLEDGMENTS. We thank Kor Brandsma, Dave Vleesenbeek, and Anneke Ditewig for biotechnical assistance and Jeannette Lorteije and Matthew Self for helpful comments on the manuscript. The research leading to these results has received funding from the European Union (EU) Sixth and Seventh Framework Programs (EU IST Cognitive Systems, Project 027198, "Decisions in Motion," and Project 269921, "BrainScaleS") and a Netherlands Organization for Scientific Research–VICI and Human Frontier Science Program grant (to P.R.R.). J.P. is supported by the People Programme (Marie Curie Actions) of the EU's Seventh Framework Programme (Project 332141).

1. Desimone R, Duncan J (1995) Neural mechanisms of selective visual attention. *Annu Rev Neurosci* 18:193–222.
2. Schall JD (1995) Neural basis of saccade target selection. *Rev Neurosci* 6(1):63–85.
3. Goldberg ME, Bruce CJ (1985) Cerebral cortical activity associated with the orientation of visual attention in the rhesus monkey. *Vision Res* 25(3):471–481.
4. Marrocco RT (1978) Saccades induced by stimulation of the frontal eye fields: Interaction with voluntary and reflexive eye movements. *Brain Res* 146(1):23–34.
5. Schiller PH, Sandell JH (1983) Interactions between visually and electrically elicited saccades before and after superior colliculus and frontal eye field ablations in the rhesus monkey. *Exp Brain Res* 49(3):381–392.
6. Bruce CJ, Goldberg ME (1985) Primate frontal eye fields. I. Single neurons discharging before saccades. *J Neurophysiol* 53(3):603–635.
7. Bruce CJ, Goldberg ME, Bushnell MC, Stanton GB (1985) Primate frontal eye fields. II. Physiological and anatomical correlates of electrically evoked eye movements. *J Neurophysiol* 54(3):714–734.
8. Wardak C, Ibos G, Duhamel JR, Olivier E (2006) Contribution of the monkey frontal eye field to covert visual attention. *J Neurosci* 26(16):4228–4235.
9. Monosov IE, Thompson KG (2009) Frontal eye field activity enhances object identification during covert visual search. *J Neurophysiol* 102(6):3656–3672.
10. Ekstrom LB, Roelfsema PR, Arsenault JT, Bonmassar G, Vanduffel W (2008) Bottom-up dependent gating of frontal signals in early visual cortex. *Science* 321(5887):414–417.
11. Moore T, Armstrong KM (2003) Selective gating of visual signals by microstimulation of frontal cortex. *Nature* 421(6921):370–373.
12. Gregoriou GG, Gotts SJ, Zhou H, Desimone R (2009) High-frequency, long-range coupling between prefrontal and visual cortex during attention. *Science* 324(5931):1207–1210.
13. Zhou H, Desimone R (2011) Feature-based attention in the frontal eye field and area V4 during visual search. *Neuron* 70(6):1205–1217.
14. Herrington TM, Assad JA (2010) Temporal sequence of attentional modulation in the lateral intraparietal area and middle temporal area during rapid covert shifts of attention. *J Neurosci* 30(9):3287–3296.
15. Hochstein S, Ahissar M (2002) View from the top: Hierarchies and reverse hierarchies in the visual system. *Neuron* 36(5):791–804.
16. Buffalo EA, Fries P, Landman R, Liang H, Desimone R (2010) A backward progression of attentional effects in the ventral stream. *Proc Natl Acad Sci USA* 107(1):361–365.
17. Mehta AD, Ulbert I, Schroeder CE (2000) Intermodal selective attention in monkeys. I: Distribution and timing of effects across visual areas. *Cereb Cortex* 10(4):343–358.
18. Egly R, Driver J, Rafal RD (1994) Shifting visual attention between objects and locations: Evidence from normal and parietal lesion subjects. *J Exp Psychol Gen* 123(2):161–177.
19. Duncan J (1984) Selective attention and the organization of visual information. *J Exp Psychol Gen* 113(4):501–517.
20. Wannig A, Stanisor L, Roelfsema PR (2011) Automatic spread of attentional response modulation along Gestalt criteria in primary visual cortex. *Nat Neurosci* 14(10):1243–1244.
21. Scholte HS, Spekreijse H, Roelfsema PR (2001) The spatial profile of visual attention in mental curve tracing. *Vision Res* 41(20):2569–2580.
22. Houtkamp R, Spekreijse H, Roelfsema PR (2003) A gradual spread of attention during mental curve tracing. *Percept Psychophys* 65(7):1136–1144.
23. Roelfsema PR, Lamme VA, Spekreijse H (1998) Object-based attention in the primary visual cortex of the macaque monkey. *Nature* 395(6700):376–381.
24. Serences JT, Yantis S (2006) Selective visual attention and perceptual coherence. *Trends Cogn Sci* 10(1):38–45.
25. Corbetta M, Shulman GL (2002) Control of goal-directed and stimulus-driven attention in the brain. *Nat Rev Neurosci* 3(3):201–215.
26. Roelfsema PR (2006) Cortical algorithms for perceptual grouping. *Annu Rev Neurosci* 29:203–227.
27. Khayat PS, Pooresmaeili A, Roelfsema PR (2009) Time course of attentional modulation in the frontal eye field during curve tracing. *J Neurophysiol* 101(4):1813–1822.
28. Roelfsema PR, Lamme VA, Spekreijse H (2004) Synchrony and covariation of firing rates in the primary visual cortex during contour grouping. *Nat Neurosci* 7(9):982–991.
29. Roelfsema PR, Spekreijse H (2001) The representation of erroneously perceived stimuli in the primary visual cortex. *Neuron* 31(5):853–863.
30. Bichot NP, Thompson KG, Chenchal Rao S, Schall JD (2001) Reliability of macaque frontal eye field neurons signaling saccade targets during visual search. *J Neurosci* 21(2):713–725.
31. Thompson KG, Bichot NP (2005) A visual salience map in the primate frontal eye field. *Prog Brain Res* 147:251–262.
32. Katsuki F, Constantinidis C (2012) Early involvement of prefrontal cortex in visual bottom-up attention. *Nat Neurosci* 15(8):1160–1166.
33. Lennie P (1981) The physiological basis of variations in visual latency. *Vision Res* 21(6):815–824.
34. Maunsell JH, Gibson JR (1992) Visual response latencies in striate cortex of the macaque monkey. *J Neurophysiol* 68(4):1332–1344.
35. Buschman TJ, Miller EK (2007) Top-down versus bottom-up control of attention in the prefrontal and posterior parietal cortices. *Science* 315(5820):1860–1862.
36. Bosking WH, Zhang Y, Schofield B, Fitzpatrick D (1997) Orientation selectivity and the arrangement of horizontal connections in tree shrew striate cortex. *J Neurosci* 17(6):2112–2127.
37. Gold JI, Shadlen MN (2007) The neural basis of decision making. *Annu Rev Neurosci* 30:535–574.
38. Poort J, Roelfsema PR (2009) Noise correlations have little influence on the coding of selective attention in area V1. *Cereb Cortex* 19(3):543–553.
39. Cohen JY, et al. (2007) Difficulty of visual search modulates neuronal interactions and response variability in the frontal eye field. *J Neurophysiol* 98(5):2580–2587.
40. Mitchell JF, Sundberg KA, Reynolds JH (2009) Spatial attention decorrelates intrinsic activity fluctuations in macaque area V4. *Neuron* 63(6):879–888.
41. Herrero JL, Gieselmann MA, Sanayei M, Thiele A (2013) Attention-induced variance and noise correlation reduction in macaque V1 is mediated by NMDA receptors. *Neuron* 78(4):729–739.
42. Buschman TJ, Miller EK (2009) Serial, covert shifts of attention during visual search are reflected by the frontal eye fields and correlated with population oscillations. *Neuron* 63(3):386–396.
43. Moro SI, Tolboom M, Khayat PS, Roelfsema PR (2010) Neuronal activity in the visual cortex reveals the temporal order of cognitive operations. *J Neurosci* 30(48):16293–16303.

Supporting Information

Pooresmaeili et al. 10.1073/pnas.1316181111

Example Simultaneous Recording in V1 and FEF

Fig. S1*A* shows the responses of an example frontal eye fields (FEF) neuron evoked by the easy, intermediate, and difficult stimuli, and Fig. S1*B* illustrates the simultaneously recorded responses of a primary visual cortex (V1) multiunit recording site. The receptive field of the FEF and V1 neurons fell on the same curve. We compared the activity evoked by the target curve (Fig. S1*A*, *Top*) to the responses evoked by the distractor (Fig. 1*A*). The appearance of the stimulus in the receptive field (RF) evoked a strong visual response in FEF with a latency of 60 ms and also in area V1 with a latency of 52 ms (as determined with a curve-fitting method; see below). We examined how the strength and latency of the attentional response modulation depended on task difficulty. In the example FEF cell, the modulation index (MI) was 1.70 in the easy condition and 1.72 in the intermediate condition, and it decreased to 1.03 in the difficult condition. Attentional modulation was weaker at the V1 multiunit recording site with an MI of 0.2 in the easy condition that decreased to 0.06 and 0.05 in the intermediate and difficult conditions, respectively. It can be seen in Fig. S1 that V1 maintained a representation of the distractor curve, whereas the representation of this curve was largely suppressed in FEF.

For the FEF cell, the latency of the attentional modulation increased from 155 ms in the easy condition to 190 ms in the intermediate condition and to 280 ms in the difficult condition. The attentional modulation latency at the V1 recording site also increased with task difficulty, from 145 ms in the easy condition to 257 ms in the intermediate condition and to 309 ms in the difficult condition. Thus, in this example recording session, the onset of attentional modulation in area V1 and FEF was delayed if the task was more difficult with latency differences between −10 ms (V1 leading FEF) and +67 ms (FEF leading V1).

Comparison of Visual and Visuomovement Neurons in FEF and V1 Recording Sites

We focused on a population of FEF neurons that included two cell types, visual and visuomovement neurons (1). We have also examined the responses of these two classes of neurons separately. To classify the cells, we used a memory-guided saccade task (1) and applied criteria based on a previous study in FEF (2) (see below for a description of this task and classification criteria). Fig. S2 shows the responses of 16 visual and 23 visuomovement cells in the curve-tracing task. The latencies of attentional modulation of the visual cells were 123, 208, and 229 ms in easy, intermediate, and difficult conditions, respectively. Average modulation latencies of visuomovement cells were 126, 169, and 224 ms in the three difficulty conditions. When we compared these latencies with V1 latencies, we did not observe significant differences at any of the task difficulty levels ($P > 0.05$, Mann–Whitney u test). Therefore, our main finding that attentional response modulation occurs at approximately the same time in V1 and FEF also holds for these two classes of FEF neurons, if analyzed separately.

Comparison of Latencies Between Multiunit Activity in FEF and V1

Our main analysis compared the latencies of V1 MUA recordings to single-unit activity in FEF. Do we obtain the same results with multiunit responses in FEF? Fig. S3 shows the MUA responses of FEF and their latencies at the three difficulty levels. The population latency of FEF multiunit response was 122 ± 39 ms (±std), 167 ± 22 ms, and 177 ± 36 ms for the easy, intermediate, and difficult condition, respectively. We did not observe a significant difference between latencies of FEF and V1 neurons in these conditions ($Ps > 0.05$, Mann–Whitney u test). Therefore, our findings are not caused by the different methods for recording neuronal activity in FEF and V1.

Influence of Firing Rate on the V1–FEF Noise Correlation

We found that the noise correlations between V1 and FEF were stronger if the RFs in the two areas fell on the target curve than if they fell on the distractor. Is this difference in noise correlation genuine, or is it related to the higher firing rates elicited by the target curve? To investigate this question we carried out a stratification procedure in which the difference in firing rate between conditions was eliminated by equalizing the number of trials across the firing rate distributions. To this end, we defined three bins of equal size between the minimum and maximum responses for every V1 recording site and also three bins for the single unit activity in the FEF (pooling across difficulty levels). Every trial of the condition with the target curve in the RFs was assigned to one of nine bins, one bin for every combination of the firing rate classes in V1 and FEF, and the same binning procedure was also used to categorize trials with the distractor in the RFs. We then equalized the firing rate distributions in the two conditions by randomly removing surplus trials from the target or distractor condition until trial number was the same in every bin. On average, 30% of trials were discarded across all pairs (between 9% and 85%), and we excluded pairs where more than half of the trials were removed from the analysis. We then repeated our analysis in the stratified data set. The average noise correlation between the remaining FEF–V1 pairs ($n = 95$) was 0.05 for responses elicited by the target curve, which was significantly larger than the noise correlation elicited by the distractor (average = 0.0065 $P < 10^{-5}$, Wilcoxon signed-rank test) (Fig. S4). Thus, the stratification analysis demonstrated that the higher noise correlation between FEF and V1 elicited by the attended curve was not caused by the stronger responses in the two areas.

SI Materials and Methods

Surgical Procedures. The details of the surgical procedures have been described elsewhere (3, 4). In short, a head-holder was implanted in a first operation which allowed head immobilization. During this first operation we also inserted a gold ring under the conjunctiva of one eye to allow the monitoring of eye position. In a second operation, arrays of 4 × 5 or 5 × 5 electrodes (Cyberkinetics Neurotechnology Systems Inc.) were chronically implanted in area V1 (right hemisphere in monkey G and left hemisphere in monkey J). In the third operation we implanted a recording chamber, on the same side as V1 arrays, above the frontal eye fields. Area FEF was localized before the surgery with MRI.

Details of the Curve-Tracing Task. The monkeys sat in a primate chair with their heads restrained, at a distance of 0.75 m from a screen. The stimuli (white curves on a black background; Fig. 1*B*) were back-projected onto the screen (70° of visual angle; 1024 × 768 pixels) by a video projector in combination with a Texas Instruments Graphics Architecture graphics board running at a frame rate of 72 Hz. A trial started as soon as the monkey's eye position was within a 1–1.5° square window centered on a 0.2° fixation point (FP). After 300 ms, the stimulus appeared (Fig. 1*A*), but the monkey had to maintain steady fixation. Correct responses were rewarded with a drop of apple juice. If the monkey broke fixation before FP offset, the trial was

terminated and discarded. The monkeys were experienced in the curve-tracing task and received additional training with the varying luminance before the recording sessions.

Memory-Guided Saccade Task. This task was used to classify FEF neurons as visual visuomovement or movement cells. After a fixation epoch (300 ms), a probe stimulus (circle) appeared on the screen and stayed in view for 100 ms. Monkeys were required to maintain fixation during an additional 400 ms (delay period) after the disappearance of the stimulus. Thereafter, two saccade targets were displayed, one at the same location as the probe stimulus and the other at the mirror location relative to the fixation point. Monkeys made a saccade toward the remembered location of the probe. We either placed the probe stimulus in the neuron's RF (as determined online by radial tuning and eccentricity tasks) or at the mirror location.

We measured visually driven activity in a time window between 50 and 150 ms after the stimulus onset and baseline activity in a 150-ms window before stimulus onset. Movement-related responses were measured in a time window between 100 ms before and 20 ms after the initiation of the saccade, whereas a presaccadic baseline was determined during the memory delay, between 350 ms and 200 ms before the initiation of the saccade. A neuron was classified as visual if the visual response was significantly greater than baseline activity (Wilcoxon signed-rank test, $P < 0.05$) and if the movement response was not significantly greater than the presaccadic baseline activity (Wilcoxon signed-rank test, $P > 0.05$). A neuron was classified as visuomovement if visual and movement responses were both significantly larger than their respective baselines (Wilcoxon signed-rank test, $P < 0.05$). For 4 out of 43 neurons, we could not record the responses in a memory-guided saccade task, because the isolation of the single neuron was lost after recordings in the main curve-tracing task. These cells were not included in the analysis above that separated visual cells from visuomovement cells.

Recording of Neuronal Activity, Eye Position, and Data Analysis. The monkey's eye position was monitored with a double magnetic induction technique (sampling rate of 1 kHz). We simultaneously recorded extracellular activity of neurons in area V1 and FEF. In area V1, spiking activity was recorded from chronically implanted multielectrode arrays with Tucker–Davis Technologies multichannel recording equipment. As in previous studies (5–9), the signals from the electrodes were amplified, band-pass filtered (500–5000 Hz), full-wave rectified, and then low-pass filtered at 500 Hz and sampled at a rate of 763 Hz. The MUA represents the pooled activity of a number of single units in the vicinity of the tip of the electrode. The population response obtained with this method is therefore expected to be identical to the population response obtained by pooling across single units. A recent study demonstrated that the MUA signal indeed provides a reliable estimate of the average single-unit response (10). After the postoperative recovery, we first measured the dimensions of the V1 receptive fields by determining the onset and offset of the visual response to a slowly moving light bar, for each of eight movement directions (10). The median area of V1 receptive fields was 0.35 deg^2 (range 0.11–4.2 deg^2), and the eccentricity ranged from 1.03° to 5.46° with a median of 3°.

The responses of single neurons in area FEF were recorded with tungsten electrodes (FHC, impedance ∼2 MΩ), which were lowered through the dura with a hydraulic microdrive (Narishige). Spikes were detected if they crossed a threshold that was determined by the experimenter. Spikes were sorted offline using the MClust toolbox (MClust 3.4, A. D. Redish) in MATLAB. Upon isolation of a neuron, we first mapped its response field by presenting saccade targets at various directions and eccentricities, as described elsewhere (3). To monitor FEF activity in the curve tracing task, we positioned one of the circular saccade targets near the center of the neuron's RF. The other circle was positioned outside the RF, at an angle of ∼90°. One of the curves fell in the receptive fields of the V1 neurons. At the end of the recording session, we usually confirmed that the electrode penetration was in FEF with intracortical microstimulation (biphasic current pulses, 100-ms train duration, 200 Hz). The penetration was considered to be in FEF if a saccade could be triggered using currents that were <100 μA (usually <50 μA).

Estimation of the Latency of the Visual Response and Attentional Modulation. We estimated the latency of attentional modulation by fitting a function $f(t)$ (Eq. **1**) to the difference in response evoked by the target and distractor curve. For the fitting of the visual response we used a more complex curve (3) that exhibits a peak and then reaches a lower sustained level:

$$f(t) = d \cdot Exp\left(\mu\alpha + 0.5\sigma^2\alpha^2 - \alpha t\right) \cdot G\left(t, \mu + \sigma^2\alpha, \sigma\right) + c \cdot G(t, \mu, \sigma). \quad \textbf{[S1]}$$

The shape of this function is determined by five parameters, μ, σ, α, c, and d; $G(t, \mu, \sigma)$ is a cumulative Gaussian. The latency of the visual response was defined as the point in time where the fitted function reached 33% of its maximum. We computed a 95% confidence interval for the latency of the visual and attentional response modulation with a bootstrapping procedure. If there are N recording sites, we randomly selected N sites with replacement and determined the latency using the curve-fitting method described above. We repeated this procedure 10,000 times to estimate the 95% confidence interval.

Computation of Noise Correlations. Noise correlations between FEF and V1 neurons (interareal correlations) and between pairs of V1 recording sites (intraareal correlations) were computed as follows. We measured the response strength in each trial by counting the number of spikes in FEF and by measuring the amplitude of the MUA response in V1 in a time window from 200 to 500 ms after stimulus onset. To compute the noise correlation, we combined data of the different difficulty levels. We removed the possible influence of differences in firing rates between difficulty levels by first z-scoring the single trial responses within difficulty levels, and then we computed the Pearson correlation coefficient of the z scores pooled across difficulty levels (Fig. 5). We applied a Wilcoxon signed-rank test to measure the significance of differences in correlation between conditions.

1. Bruce CJ, Goldberg ME (1985) Primate frontal eye fields. I. Single neurons discharging before saccades. *J Neurophysiol* 53(3):603–635.
2. Gregoriou GG, Gotts SJ, Desimone R (2012) Cell-type-specific synchronization of neural activity in FEF with V4 during attention. *Neuron* 73(3):581–594.
3. Khayat PS, Pooresmaeili A, Roelfsema PR (2009) Time course of attentional modulation in the frontal eye field during curve tracing. *J Neurophysiol* 101(4):1813–1822.
4. Roelfsema PR, Lamme VA, Spekreijse H (1998) Object-based attention in the primary visual cortex of the macaque monkey. *Nature* 395(6700):376–381.
5. Cohen MR, Maunsell JH (2009) Attention improves performance primarily by reducing interneuronal correlations. *Nat Neurosci* 12(12):1594–1600.
6. Logothetis NK, Pauls J, Augath M, Trinath T, Oeltermann A (2001) Neurophysiological investigation of the basis of the fMRI signal. *Nature* 412(6843):150–157.
7. Roelfsema PR, Lamme VA, Spekreijse H (2004) Synchrony and covariation of firing rates in the primary visual cortex during contour grouping. *Nat Neurosci* 7(9):982–991.
8. Roelfsema PR, Tolboom M, Khayat PS (2007) Different processing phases for features, figures, and selective attention in the primary visual cortex. *Neuron* 56(5):785–792.
9. Xing D, Yeh CI, Shapley RM (2009) Spatial spread of the local field potential and its laminar variation in visual cortex. *J Neurosci* 29(37):11540–11549.
10. Super H, Roelfsema PR (2005) Chronic multiunit recordings in behaving animals: Advantages and limitations. *Prog Brain Res* 147:263–282.

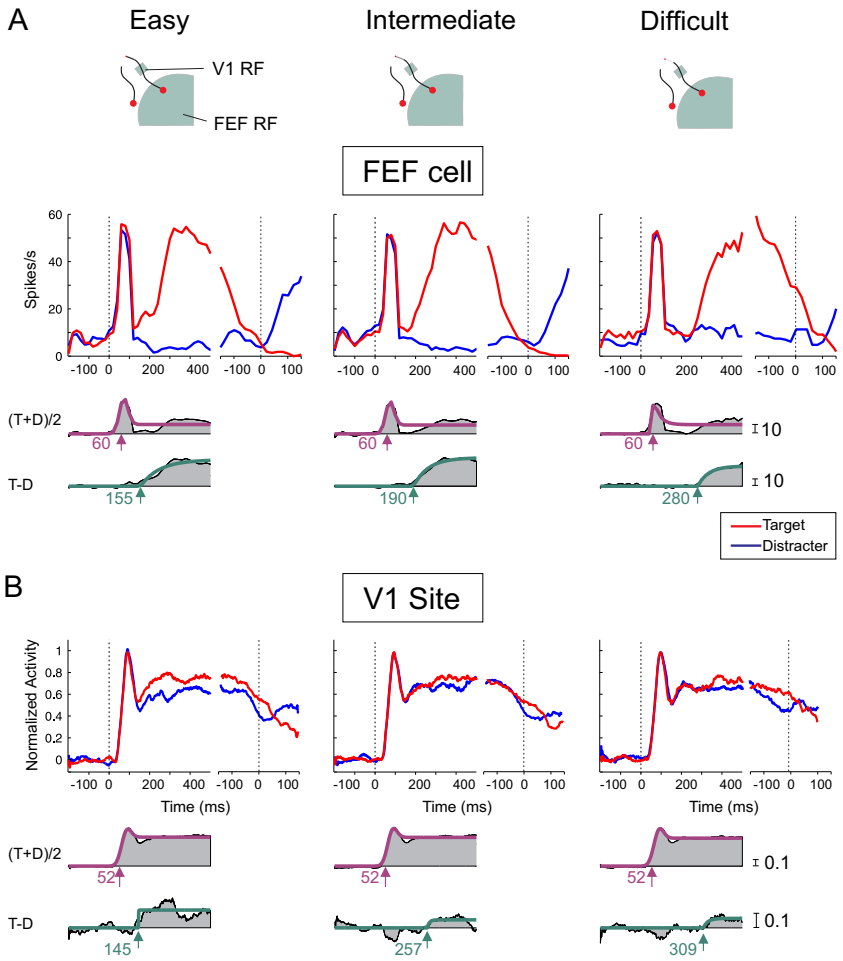

Fig. S1. Example simultaneous recording from FEF area V1. (*A* and *B*) Responses of an example FEF cell and a V1 recording site. (*Top*) The FEF and V1 RF relative to the stimuli. The PSTHs depict neuronal responses of the FEF cell (*A*) and the V1 neurons (*B*) evoked by stimuli at the three levels of difficulty. The red and blue traces show the responses evoked by the target and distractor curve, respectively. In both *A* and *B*, *Lower* panels show the visual response [averaged across target and distractor curve (T + D)/2] and the attentional response modulation (T − D). Purple and green curves were fitted to estimate the latency of the visual response and the response modulation, respectively. On the right side of the graphs, PSTHs have been aligned on the saccade onset, defined as the moment when the monkey's gaze left the fixation window (dashed line).

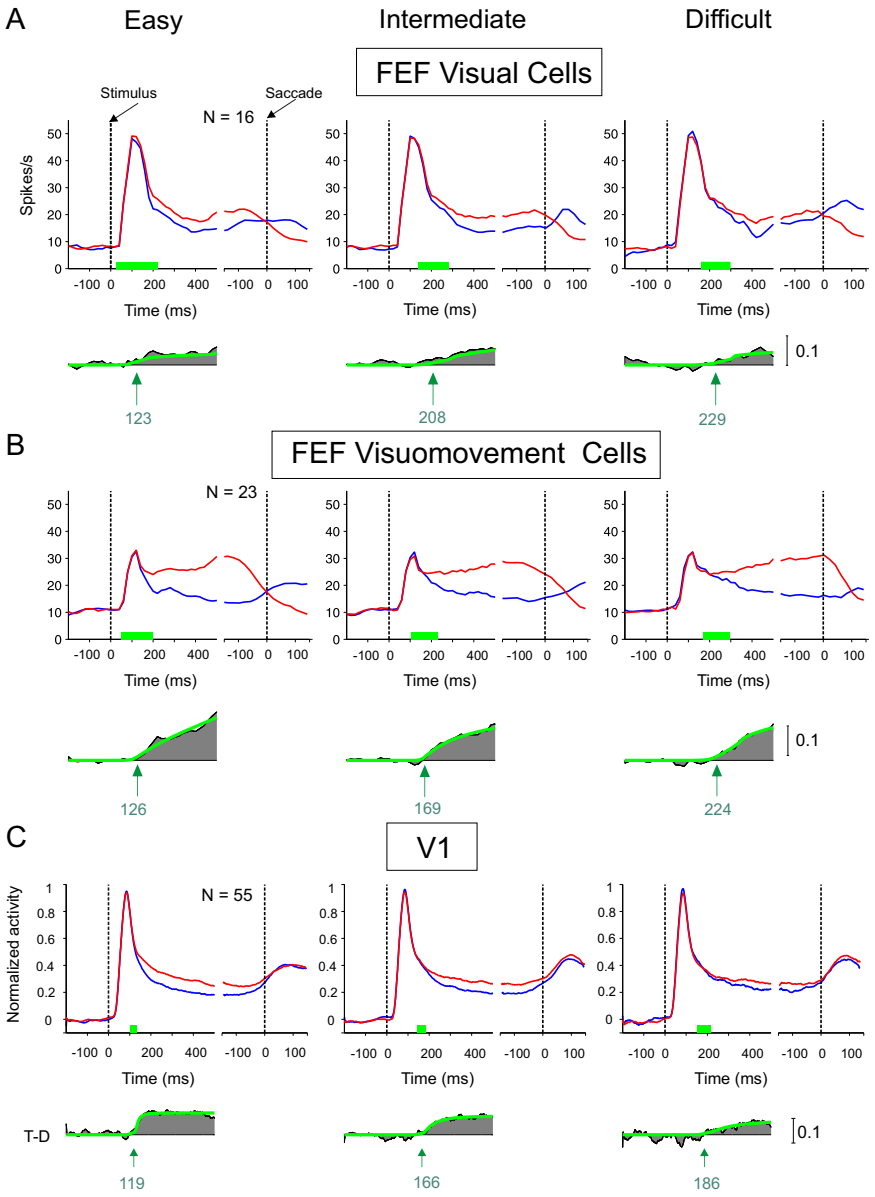

Fig. S2. Activity of visual and visuomovement neurons in FEF and comparison with area V1. The red and blue traces show the responses evoked by the target and distractor curve, respectively, for visual neurons (*A*) and visuomovement neurons (*B*) in FEF and recording sites in area V1 (*C*). In *A*–*C*, *Lower* panels show the attentional response modulation. Curves were fitted to estimate the latency of the response modulation (green). Rectangles on the *x* axis show the mean estimate ±s.d. (determined with bootstrapping). On the right side of the graphs, the PSTHs were aligned on the saccade onset.

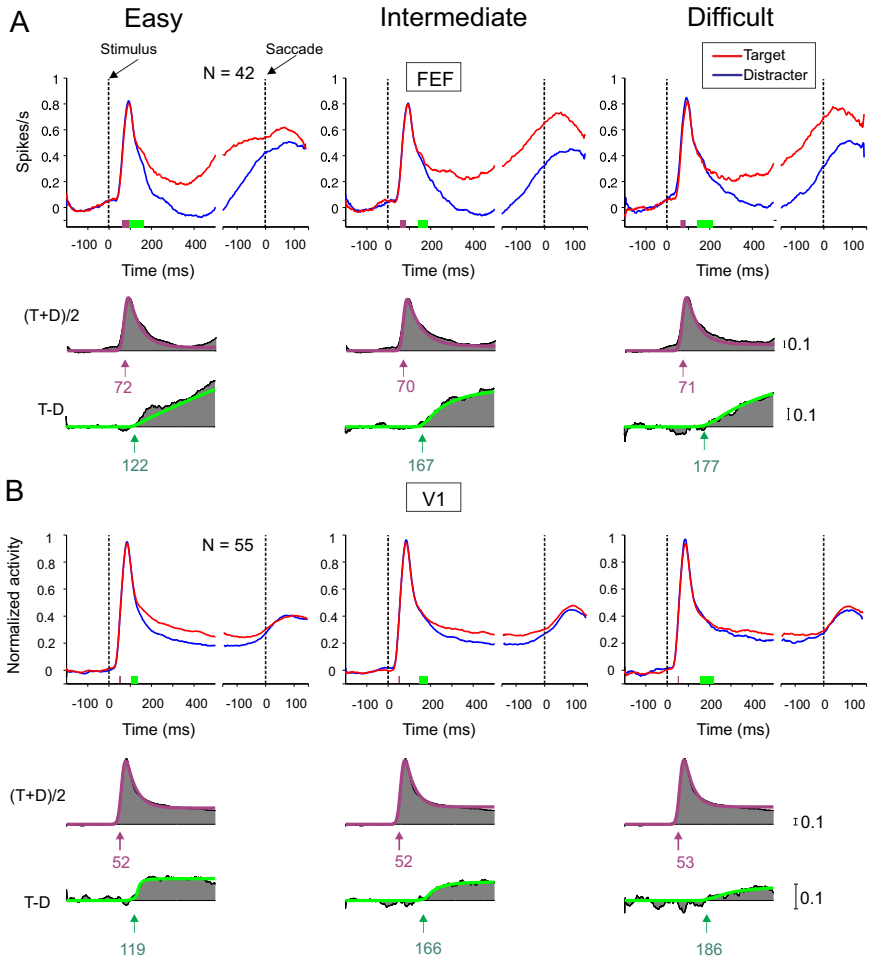

Fig. S3. Population multiunit responses in FEF and area V1. Average responses of all FEF MUA recordings (*A*) and area V1 MUA recordings (*B*). All conventions are as in Fig. S2.

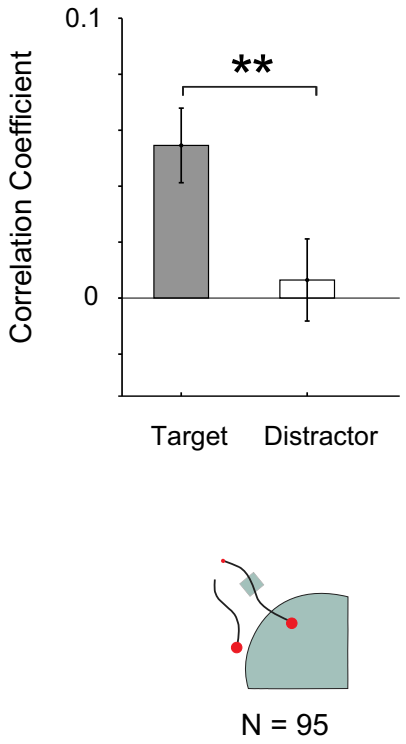

Fig. S4. Noise correlations between FEF and V1 after stratification to equalize response magnitudes. Bars show noise correlation between FEF and V1 evoked by the target curve (gray) and distractor curve (white). $^{**}P < 0.0001$.